Internship report:
Exploring methods to determine the impact of instrumental systematic errors on PeVatron detection with the Cherenkov Telescope Array

Emma Carli
emma.carli@outlook.com
Centre de Physique des Particules de Marseille
9 week internship in the CTA group

August 26, 2019

Abstract

This project aimed at determining the impact of instrumental systematic errors on PeVatron detection with the Cherenkov Telescope Array. To do so, the latter's response is modified to emulate the influence of systematics, using guidelines from Graham et al. [2018]. This is done with the Effective Area response component and a method is suggested for the Energy Dispersion component. From this, PeVatron data is simulated and fitted in the aim of comparing spectral parameters retrieved with different responses. This is left unfinished and leads are suggested to complete the analysis.

Contents

1 Introduction

This internship report was written after a 9-week stay in the CTA groupe at CPPM, Marseille. I worked under the supervision of Dr. Franca Cassol, with the assistance of the rest of the CTA astrophysicists there - head of group Dr. Costantini, postdoctoral student Dr. Anguner and PhD student Gaia Verna. The production of this project is left available in the group's internal files.

The PeVatron groups works on the future detection of PeVatrons with the Cherenkov Telescope Array, and I joined this research during the summer following my first year of astrophysics Master's at the University of Glasgow.

In the following section, I introduce the context and the aim of this project. In section 3, I detail the methods I employed: I modified the CTA response, with which I simulated and analysed PeVatron data. I discuss how to continue this project in section 4.

2 Background

When a high energy cosmic ray or gamma-ray enters the Earth's atmosphere, it produces a particle shower. The relativistic particles exceed the speed of light in air. This produces a blue flash of Cherenkov light. Since these high energy sources have low fluxes, a ground-based array has the advantage of a higher collection area than a space-based telescope.

The Cherenkov Telescope Array (hereafter CTA) is a project which will be constructed in the Atacama desert, Chile and La Palma, Spain. Its large mirrors and photomultipliers will detect the faint Cherenkov light from particles and gamma-rays of astrophysical origin. It will observe at higher energies than its Cherenkov telescope predecessors.

This study focuses on gamma-ray observations, the primary focus of CTA. Since cosmic rays are charged particles, their path from the source to Earth is deflected by electromagnetic forces and its spatial origin cannot be determined - only its energy. Gamma-rays observation therefore provide extra information.

One of CTA's Key Science Projects is to determine the position of galactic PeVatrons. These are, for example, shock fronts or magnetic fields that accelerate cosmic rays to petaelectronvolt energies. To do so, the gamma rays resulting from this acceleration are detected.

Above 10 TeV, the gamma rays cannot be emitted by inverse Compton from accelerated electrons [Aharonian, 2013]. They result from accelerated hadrons (protons and nuclei) which lose energy to the interstellar medium. The gamma rays are about 10 times less energetic than the parent particle. We are therefore looking in the 100 TeV range for PeVatrons.

So far, only one PeVatron has been identified, by CTA's predecessor HESS (the High Energy Stereoscopic System), near the galactic centre [The H.E.S.S Collaboration, 2016]. CTA is the first gamma-ray telescope to detect above tens of TeV (up to 300), and should therefore detect many more. This project is part of this search: I explored methods to determine the impact of the instrument, in particular systematic errors, on these detections. In the following section, I describe these methods.

3 Methods

To estimate the effect of the telescope systematics on PeVatron detections, I bracketed the CTA IRFs, simulated PeVatron observations with this modified response, and examined the model fitted to it using CTA data analysis.

3.1 Bracketing

Since CTA is not constructed yet, there are putative Instrument Response Functions provided for the arrays. They contain the following components, all as a function of true energy of the observed event and angle between source and pointing (the offset angle):

- Effective Area (AEff) of the array, in m^2,
- Energy Dispersion (EDisp): a probability density function (PSF) of the energy migration (ratio of reconstructed to true energy of the event);
- Point Spread Function (PSF);
- Background acceptance: an assumed spectral flux density of detected background events (i.e. unrelated to the observed source).

I investigated methods to apply modifications emulating instrumental systematic errors to these IRFs. I followed the guidelines in Graham et al. [2018]. From CTA requirements, they suggest sytematic error values and functions to apply to the IRFs - the process is coined ‘bracketing’. I chose to apply systematics to the AEff and EDisp components with error functions dependent on the true energy of the events.

I first had to choose an IRF to apply the modifications to. I chose the Southern (Chile) array as the projected North array layout is not capable of detecting in hundreds of TeV. I chose the latest IRF production, *prod3b-v2*. I discarded the lowest altitude pointing IRFs because they had no data in background acceptance at high energies and low offsets, a parameter space particularly useful to this project. I picked the longest exposure to replicate a deep CTA observation of a pre-detected PeVatron. My final choice was therefore the *prod3b-v2*, azimuth 40 degrees, 40h IRF (figure 1).

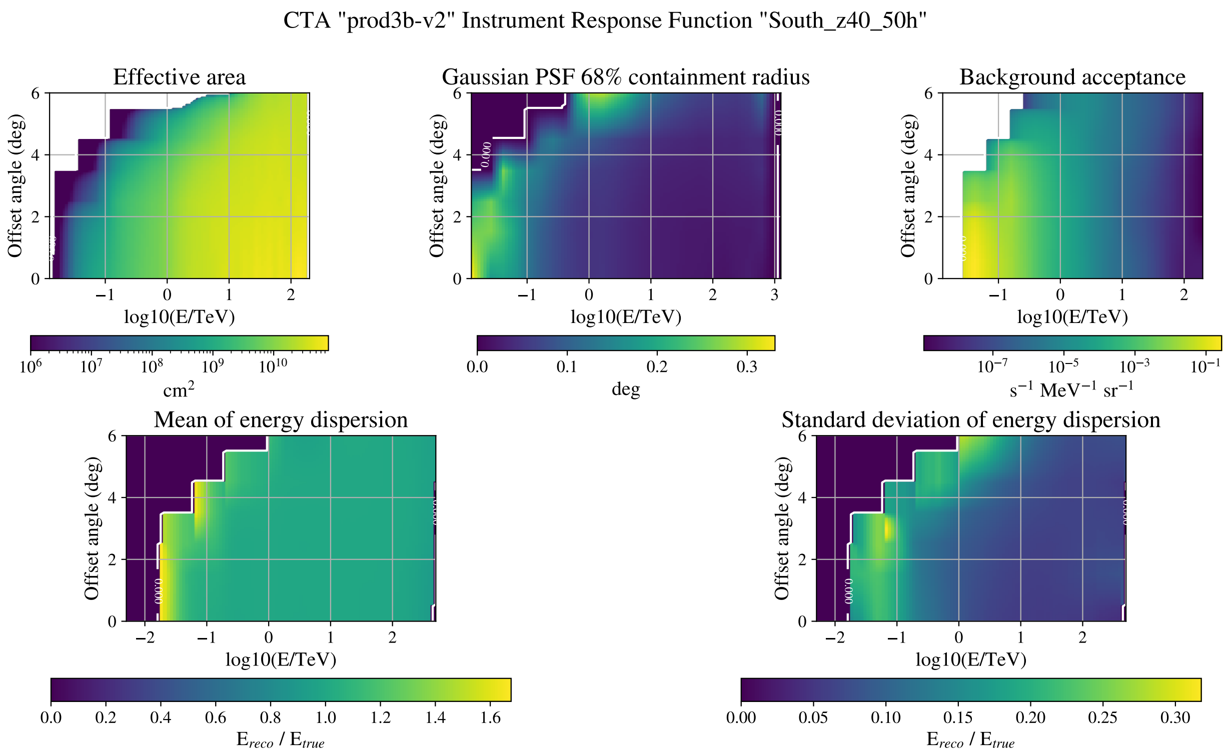

Figure 1: The IRF I chose for modifications.

3.1.1 Effective Area

I thus began modifying the Effective Area component of this IRF. The `cta-irf-scaling` program was written for the CTA Consortium by Dr. Ievgen Vovk as part Graham et al. [2018]. It implements IRF Effective Area bracketing. The guideline from Graham et al. [2018] is to introduce systematic errors by scaling the effective area by 5% using the following error functions: a plus or minus constant bracketing, a ascending or descending gradient over the energy range, and a step function representing transitions between different sizes of telescopes in the array.

This was rather easily implemented with `cta-irf-scaling`. I input the energy range over which to bracket (the same as for simulations, section 3.2), the error function and scale. I saved the IRF as a standalone rather than in the original IRF folder for better compatibility with `ctools`, a CTA data analysis package, used in 3.2 and 3.3 [Knödlseder et al., 2016]. I also included different plotting and an if statement for an EDisp column name which has been changed between productions. The results are shown in figure 2.

3.1.2 Energy Dispersion

The AEff bracketing being functional, I began examining the Energy Dispersion IRF component. It consists of a probability density function (PDF) of energy migration/dispersion ratio ($\frac{E_{\text{reco}}}{E_{\text{true}}}$) defined over a grid of offset angles and true event energy. An illustration of it is shown in figure 3 and the values of the last two plots in figure 1 are drawn from this PDF. These are the two constituents of the Energy Dispersion IRF that can be bracketed: the energy resolution (the widths of migration ratio PDFs at each given true energy and offset angle, or energy dispersion standard deviation) and scale (the migration ratios to which the PDFs are attributed). I only looked at the energy scale in this project due to time constraints.

In the systematics guidelines document, Graham et al. [2018], a 6% relative error is inferred from the CTA requirement *PROG-0100 Systematic Energy Uncertainty*, which applies to 'systematic errors or biases in the energy of reconstructed gamma-ray photons'. I could not determine whether the error is relative to the true energy of the incoming event (E_{true}) or the reconstructed energy (E_{reco}). It could be (taking a positive constant error function, for example):

$$\frac{E_{\text{reco}} + 6\% \cdot E_{\text{true}}}{E_{\text{true}}} = \frac{E_{\text{reco}}}{E_{\text{true}}} + 0.06 \tag{1}$$

or

$$\frac{E_{\text{reco}} + 6\% \cdot E_{\text{reco}}}{E_{\text{true}}} = \frac{E_{\text{reco}}}{E_{\text{true}}} \cdot 1.06 \tag{2}$$

These options were suggested by Dr. Cassol. I chose the second option (although the first is most probably better since the IRF components are a function of true event energy).

I tried applying the energy scale bracketing using `cta-irf-scaling`, but the mean of energy dispersion of the modified IRFs, such as plotted in figure 1, was left unchanged. Looking into the problem, I realised the program only scaled the PDF values by the input percentage (see figure 3), which does not modify mean or standard deviation of the energy dispersion. The values drawn from the PDF stay the same. We suggest this is a mistake.

After some unsuccessful attempts at scaling the IRF migration ratio with respect to E_{true}, I decided to simplify the approach by scaling directly the simulated data. I simply applied the error functions from `cta-irf-scaling` (the same as in 3.1.1) to the energies of the events in the simulated dataset, as shown in figure 4. This method could be a good approximation, but I applied it incorrectly. This mistake is detailed in section 3.3.

3.2 Simulations

Here I relate the simulated PeVatron observations with this modified response. The computations in this part and the next were done with the CTA data analysis software `ctools`, in development for future use in the array. I detailed the names of most of the functions used, which start with `ct` or `cs`.

I simulated PeVatrons with an exponential cutoff power law, which is the following function of energy E:

$$k_0 \left(\frac{E}{1 \text{ TeV}} \right)^{-2} \exp \left(\frac{-E}{E_{\text{cut}}} \right) \tag{3}$$

where the pivot energy is set at 1 TeV and the index at -2. E_{cut} is the cutoff energy and k_0 is the prefactor flux in photons $\text{cm}^{-2}\text{s}^{-1}\text{MeV}^{-1}$.

The characteristics of the `ctools` simulations, run with each IRF, are listed below:

- no spatial extent (point source approximation)
- energy dispersion applied
- 0.5 degree offset angle
- 0.8 degree field of view radius
- 40 hour observation

- energy minimum 100 GeV
- energy maximum set at the maximum IRF range
- fluxes at 20, 40, 60 and 80 mCrab ($3.8 \cdot 10^{-20}$ photons $\mathrm{cm}^{-2}\mathbf{s}^{-1}\mathrm{MeV}^{-1}$) to determine the influence of systematics and statistical errors
- cutoffs at 50 (not a PeVatron, used as a test for well-observed cutoff), 100 and 200 TeV
- the seed was not changed between simulations to be able to solely include systematic differences (no probability sampling or statistical errors change)
- approximately 7 times background to source area.

To this source must be added background events to simulate a realistic observation. It is possible to simulate a custom background source with `ctools`. The spatial and spectral parameters of both source and background are set using an XML file. Then these observation parameters are passed into the `ctobssim` function, which simulates both sources through the given IRF and adds statistical variations. This produces a FITS file with the summed events. This works with modified IRFs too.

Unfortunately, I did not use the right method to simulate the background in the context of my project. I used the background template in the IRF, as plotted in figure 1. In the XML source files, it is called '`CTAIrfBackground`'. This is the only `ctools` input background which does not go through the rest of the IRF components for the simulations. Therefore, modifications to the IRF components are not applied to it. The background contributing to most of the observing area, the simulations I produced with a modified AEff had only a small part of the counts bracketed (the source's). They were therefore erroneous. To solve this, I would have had to use the '`CTAAeffBackground`' or use a spectral law, building it from scratch. Sadly, this was noticed too late to fix it. This choice of background also led to incorrect energy bracketing (see section 3.3).

The background in the IRF I chose also goes to zero before the effective area does, which can be a problem in weighting source and background at high energies.

An example (non bracketed) simulation with IRF-provided background is shown in figure 5.

3.3 Data analysis

Once the bracketed data was simulated, I went on to produce a fit as the CTA pipeline will, identifying the source parameters. This was to determine changes in detected spectral features between differently bracketed IRFs.

I binned the data to reduce computing time - reducing it into 'cubes' (data files with binned energy and spatial dimensions). With `ctbin`, I set ten bins per energy decade and a 0.02 degree spatial resolution to the simulations, as advised by Dr. Anguner. I then binned the IRF response - I wasn't sure if this was only advised in the case of a stacked observation, so I proceeded with it. I computed an exposure cube (effective area multiplied by observation time), a PSF cube, a background cube, and an Energy Dispersion cube, with the amount of pixels recommended by `ctools`.

The data was thus prepared for `ctlike` likelihood fitting. This determined spectral parameters of an exponential cutoff power law. I decided to input this model in the fit, and when no cutoff was found I deemed it equivalent to fitting a simple power law. I plotted each model fit and its errors, in flux against recovered event energy, with `ctbutterfly` (see figure 6a). One way to compare this model to the data is to convert the model into counts with the IRF, using `ctmodel` and `csresspec`, which produces graphs such as figure 6b.

Another way is to re-fit the data. I used `csspec`, which computes a fit per bin, fixing all parameters to model values except for flux. This allows to create a flux spectrum with errors of the simulated data. This can be overlaid to the model for comparison (figure 6a). At very high energies, the number of events are quite low, which leads to some upper limit error bars at times. To avoid this, I tried to double the bins at this end but this decreased greatly the precision on the cutoff fit.

I next ran `cterror` to compute asymmetrical errors on the cutoffs at 95% and 68% confidence levels. I also inferred a p-value from the count residuals.

I referred in section 3.1.2 to the Energy Dispersion bracketing being unsuccessful due to a wrong choice of background simulation. This problem occurred during the fitting. To `ctlike` is provided a model with free parameters to fit for both source and background. While the source is fit as a exponential cutoff power law with no more information, the IRF background acceptance rate is passed to the function which fits a factoring power law to account for statistical variations. These changes being small, the fitted prefactor stays close to one and the index is near zero. Therefore, if I shift the energies of all events, the source fit will have enough freedom to account for it, but the background fit will be tied to what is provided (and not bracketed) in the IRF, producing a inaccurate fit with significantly lower p-values. Still, the AEff bracketing fits were also incorrect since the background counts were left unbracketed.

In any case, without any bracketing there seemed to be a problem with my fits. The residuals, when plotted in counts, looked correlated as appears in figure 6b, with or without bracketing. Removing the background did not change this, although plotting in sigma removed this correlation. Further, the p-values were quite low, with or without bracketing, unless the background was removed.

4 Discussion

Since this project was left unfinished, there are several points that need improved and continued. I have gathered ideas for this continuation here.

- Repeat the simulations with bracketed IRFs using an appropriate background, which will go through the modified effective area, and will have more freedom in the background model.
- Use an on/off analysis to follow Dr. Anguner's method, get faster calculations, and have a more realistic approach to the background fit. This will allow to investigate the role of the background in fit quality (p-values) and correlated residuals.
- Instead of bracketing counts post-simulation, implement IRF energy dispersion scaling in `cta-irf-scaling`, and further, energy resolution bracketing.
- Find out at which flux do systematics become more significant than statistical fluctuations.
- Make a graph overlaying the simulated sources to CTA sensitivity to give context to the analysis.

This will allow an answer to the aim of this project, which is to find how instrumental errors influence PeVatron detection.

5 Conclusion

This project aimed at determining the impact of instrumental systematic errors on PeVatron detection with the Cherenkov Telescope Array. Although I could not get to this end, I explored some methods paving the way.

I applied Effective Area bracketing following Graham et al. [2018] guidelines. I also found a potential mistake in the correspondent software `cta-irf-scaling` in Energy Dispersion bracketing, and proposed an alternative, a first approximation at Energy Dispersion scaling. I learned how to simulate and analyse CTA data with `ctools`, and finally suggested leads to finish this analysis.

This project was very instructive to me, in theory, instrumentation and software of astroparticle physics and high energy astrophysics. I thank the group for having me!

6 Acknowledgements

This research has made use of the CTA instrument response functions provided by the CTA Consortium and Observatory, see the prod3b-v2 page for more details.

The graphs in this report were produced with the CTA Consortium `ctools` [Knödlseder et al., 2016] software's plotting functions (which I have slightly modified to adapt to my needs), unless specified otherwise.

References

Felix A Aharonian. Gamma rays from supernova remnants. *Astroparticle Physics*, 43:71–80, 3 2013. URL http://dx.doi.org/10.1016/j.astropartphys.2012.08.007.

J A Graham, J Biteau, C Boisson, J Cardenzana, F Cassol, H Costantini, De Souza, E De Ona Wilhelmi, C Deil, T Hassan, W Hofmann, B Humensky, A Sokolenko, L Tibaldo, C Trichard, I Vovk, S Wagner, and R Zanin. Guidelines : systematic uncertainties of instrumental origin with CTA. 2018. URL https://docs.google.com/document/d/1oBOwOOgMcL8Shww6oLjiQoQVbOwlOHGuBTV1YGHTc_k/.

J. Knödlseder, M. Mayer, C. Deil, J. B. Cayrou, E. Owen, N. Kelley-Hoskins, C. C. Lu, R. Buehler, F. Forest, T. Louge, H. Siejkowski, K. Kosack, L. Gerard, A. Schulz, P. Martin, D. Sanchez, S. Ohm, T. Hassan, and S. Brau-Nogué. GammaLib and ctools: A software framework for the analysis of astronomical gamma-ray data. *Astronomy & Astrophysics*, 593:A1, 6 2016. URL http://dx.doi.org/10.1051/0004-6361/201628822.

The H.E.S.S Collaboration. Acceleration of petaelectronvolt protons in the Galactic Centre. *Nature*, 531 (7595):476–478, 3 2016. URL http://dx.doi.org/10.1038/nature17147.

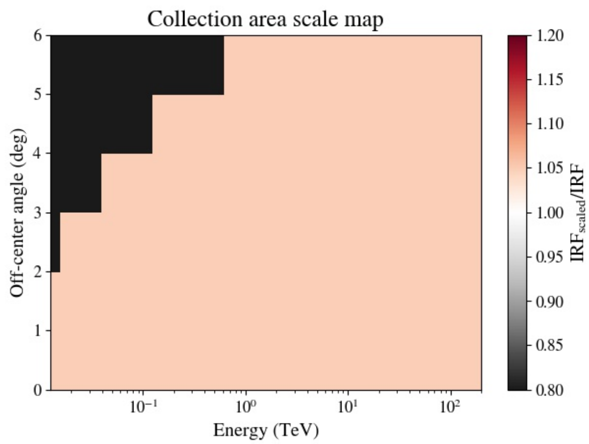

(a) Bracketing the effective area with a positive constant error function.

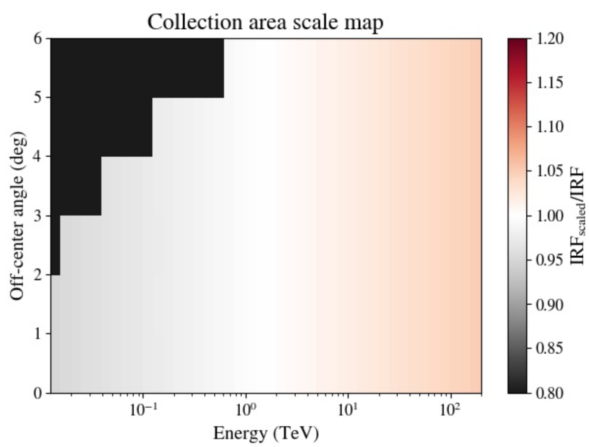

(b) Bracketing the effective area with a positive gradient error function.

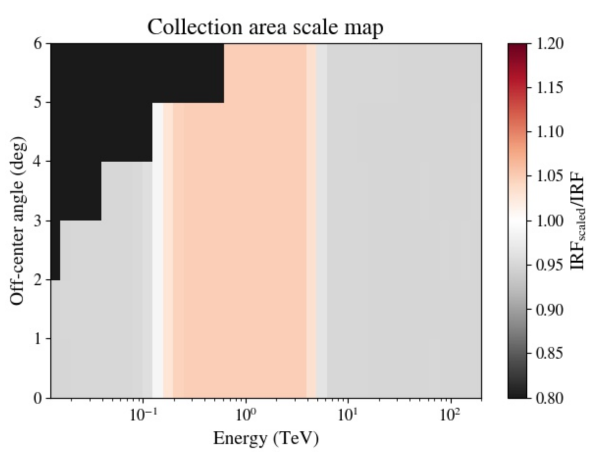

(c) Bracketing the effective area with a positive step error function, with telescope transitions at 0.15 and 5 TeV. The first transition width is of 11%, the second 6% (see Graham et al. [2018]).

Figure 2: Positive effective area bracketing. The negative bracketing is not plotted here. These graphs were produced with a slightly modified version of `cta-irf-scaling`.

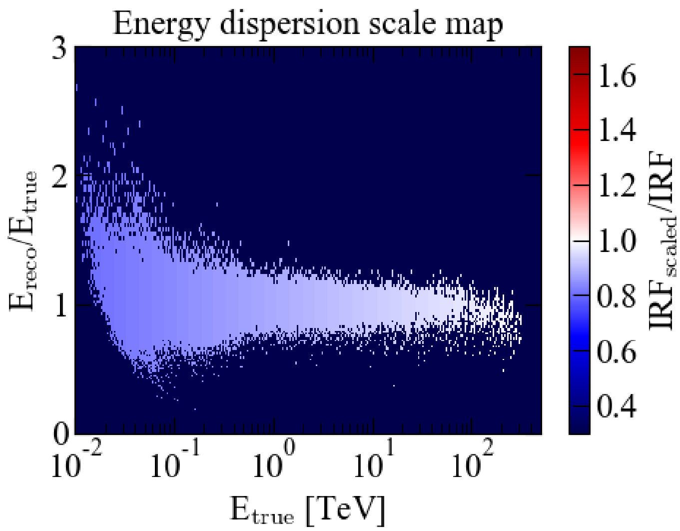

Figure 3: An example of possibly incorrect energy scaling by `cta-irf-scaling`. The Energy Dispersion component of the IRF is plotted for offset angles comprised between 0 and 1 degree. The PDFs are plotted in vertical lines on this plot, for each E_{true} bin. They are scaled (in colour, labelled IRF rather than PDF) with a positive gradient function over the E_{true} axis. Therefore, each individual PDF is scaled by a constant. This does not modify its mean and standard deviation, and the values drawn from it stay the same. Energy scaling would actually correspond to changing the shape of this distribution with respect to E_{true}, and with respect to the ratio axis for energy resolution scaling. This graph was taken from a presentation by Dr. Humberto Martinez Huerta in the 13/12/2018 CTA Physics Working Group meeting.

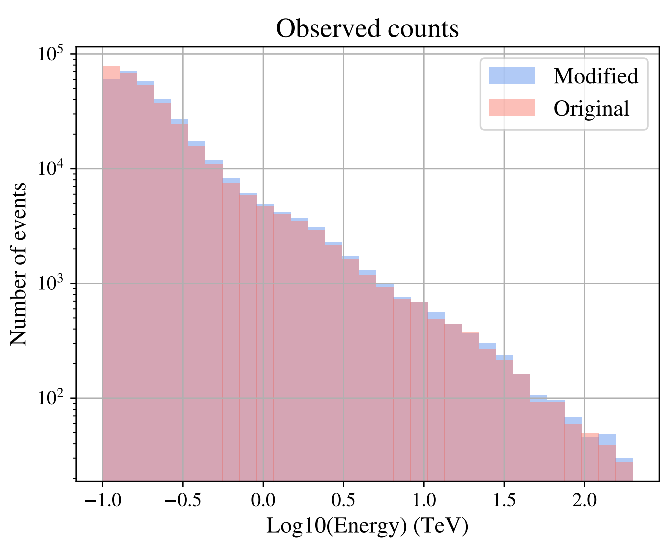

Figure 4: On this example of positive constant energy bracketing, the energy of each event is increased, which here shifts the event histogram to the right of the x-axis. Although the method could be useful, I applied it incorrectly - the mistake is explained in section 3.3.

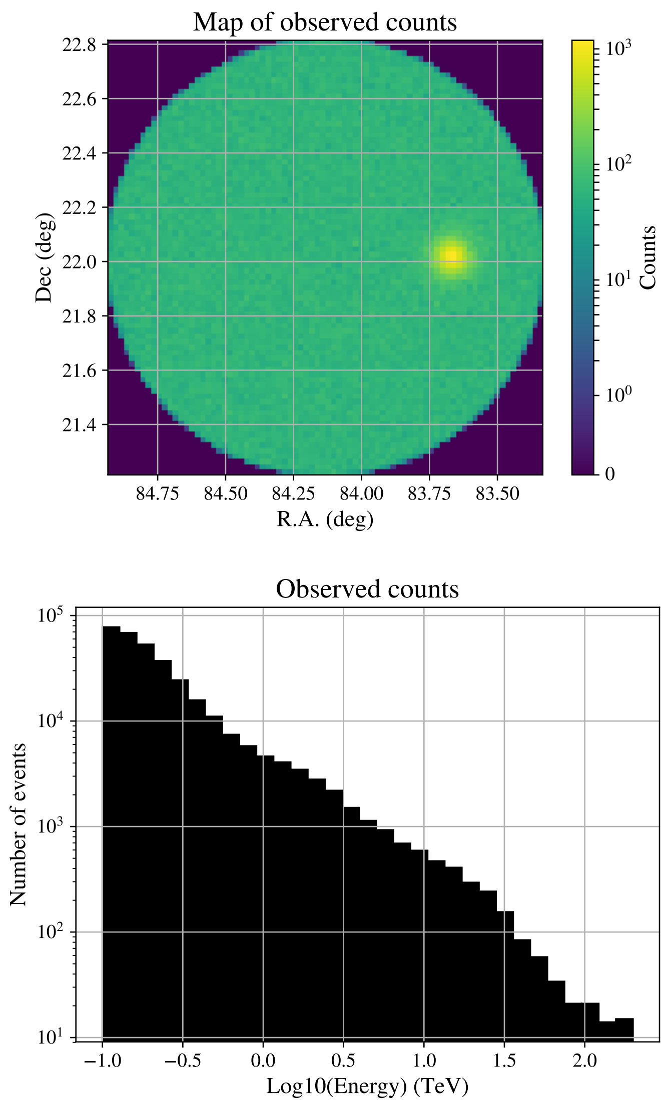

Figure 5: A simulated 80 mCrab, 50 TeV cutoff source with no bracketing.

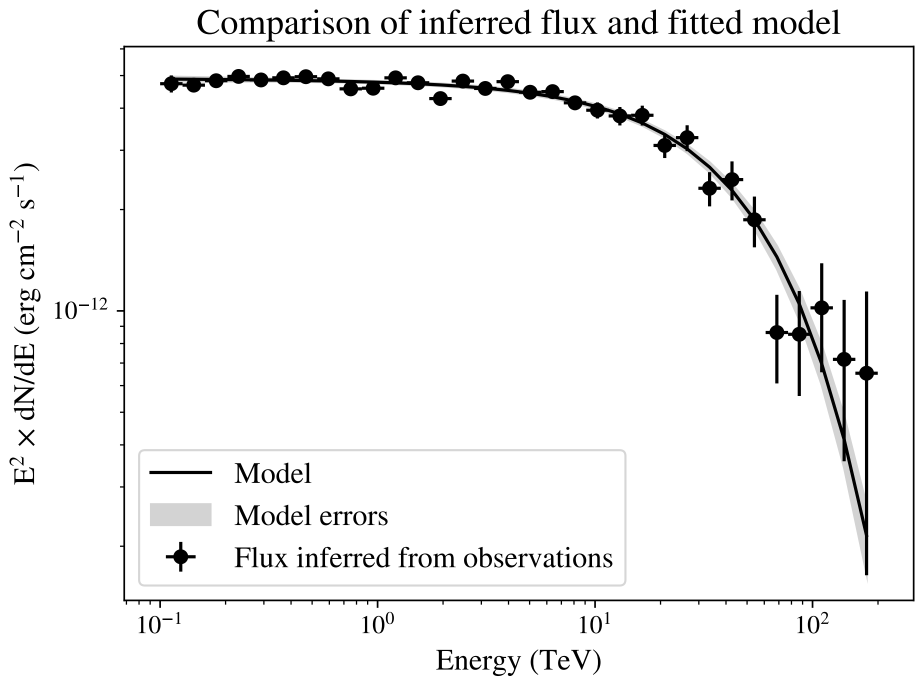

(a)

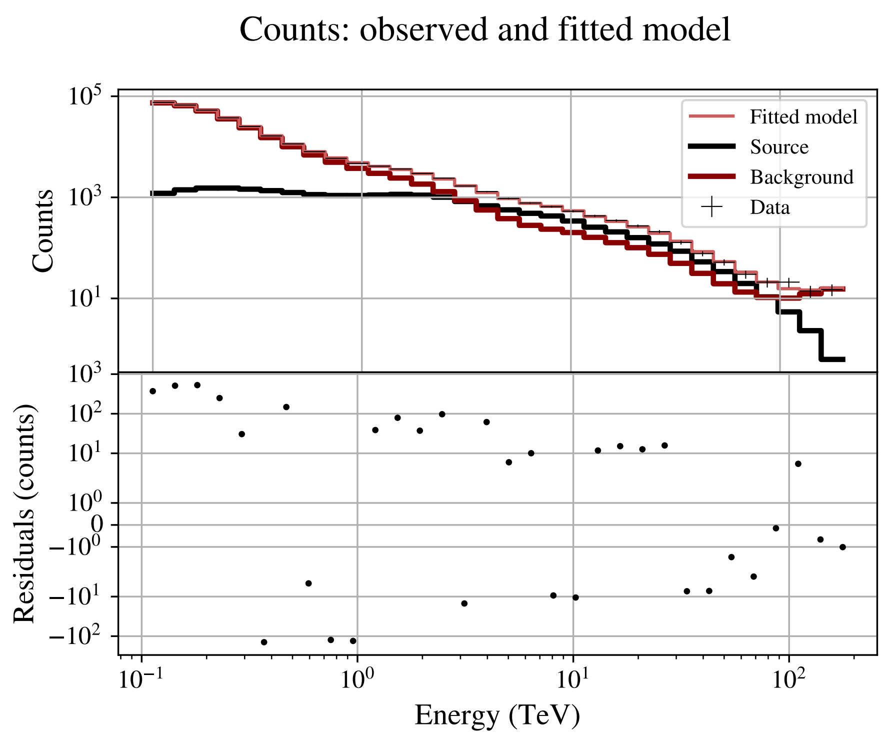

(b)

Figure 6: Data analysis and fitting on a simulated 80 mCrab, 50 TeV cutoff source with no bracketing. The residuals on the counts appear correlated.